Contents lists available at ScienceDirect

Journal of Molecular Liquids

journal homepage: www.elsevier.com

Interaction pathways of specific co-solvents with hydroxypropyl-β-cyclodextrin inclusion complexes with benznidazole in liquid and solid phase

Polyanne N. de Melo [a], Euzébio G. Barbosa [a], Claudia Garnero [b], Lilia B. de Caland [a], A.A.N. de Lima [a], Matheus F. Fernandes-Pedrosa [a], Marcela R. Longhi [b], Arnóbio Antônio da Silva-Júnior [a, *]

[a] *Pharmaceutical Technology and Biotechnology Laboratory, Department of Pharmacy, Federal University of Rio Grande do Norte (UFRN), Av. Coronel Gustavo Cordeiro de Farias s/n, Petrópolis, CEP 59012-570 Natal, RN, Brazil*

[b] *Research and Pharmaceutical Technology Development Unit (UNITEFA, CONICET-UNC) and Department of Pharmacy, Faculty of Chemical Sciences, National University of Córdoba, Ciudad Universitaria, X5000HUA Córdoba, Argentina*

ARTICLE INFO

Article history:
Received 4 March 2016
Received in revised form 23 July 2016
Accepted 12 August 2016
Available online xxx

Keywords:
Poorly water-soluble drugs
Solubility
Supramolecular aggregates
Solid dispersion
Cyclodextrins
Spray drying

ABSTRACT

The main purpose of the study was to assess the mechanism whereby the co-solvents triethanolamine (TEA) and 1-methyl-2-pyrrolidone (NMP) interacted with hydroxypropyl-beta-cyclodextrin (HP-β-CD) in ternary associations for improving the solubility and dissolution rate of the insoluble ingredient benznidazole (BNZ). In liquid phase, the solubility diagrams and Job's plot results were further explored by *in silico* molecular modeling and experimental ^{1}H NMR spectroscopy studies. The structure of the inclusion complexes in the binary and ternary association were established. The competition of NMP with the drug for the HP-β-CD cavity was evidenced, while TEA stabilized the drug-CD interactions, forming ternary complexes. FTIR analysis confirmed distinct intermolecular interactions among the compounds in the different solid dispersions prepared by physical mixture (PM) and spray drying (SD). The co-solvents improved the drug dissolution performance from PM ternary associations due to their enhanced wettability of particles changing the drug-CD interaction. In addition to the SD samples exhibiting spherical particles, the co-solvents increased the crystallinity of drug in the particles and the ternary associations did not reproduce the drug dissolution rate identified in the PM samples. The experimental results proved the importance of the co-solvents to improve the drug dissolution performance from ternary complexes and established the mechanism whereby these substances worked together with the CD in a new and promising raw material. Due to the high temperature, the spray drying was not a suitable method for preparing the specific ternary complexes.

1. Introduction

Chagas disease is caused mainly by the flagellate *Trypanosoma cruzi* that affects about 6 to 7 million people worldwide. The World Health Organization (WHO) classified it as a neglected disease due to the few alternatives of available treatment. Benznidazole (BNZ) (N-benzyl-2-(2-nitroimidazol-1-yl)) acetamide is the main drug commercially available, usually in tablet form, to treat Chagas disease. However, problems of efficacy are reported as it requires high doses of the drug, which causes side effects [1,2]. In addition, compliance in use by children and the elderly is connected with the absence of liquid dosage forms [3]. These limitations can be associated with low solubility of the BNZ, and, thus, an increase in its aqueous solubility may provide benefits in the treatment of Chagas disease through greater patient compliance to treatment.

Some strategies have been investigated for improving the apparent aqueous solubility of non-polar drugs, such as cosolvency, oral emulsions, and complexation with cyclodextrins. Nevertheless, BNZ exhibits an interesting and paradoxical behavior. The water-solubility of this substance is considered poor with a partition coefficient of about 0.9, but this drug is practically insoluble in pharmaceutical oils. Previous studies reported low drug loading in soybean oil O/W emulsions [4]. In addition, a soluble oral dose of BNZ was not achieved when several kinds of co-solvents and surfactants were tested previously [5].

Cone-shaped structured cyclodextrins (CDs) are cyclic oligosaccharides formed by (α-1,4)-linked D-glucopyranose that guarantees reduced hydrophilic behavior of the internal ethereal oxygen of glucose residues, while the outer hydroxyl groups contribute to water solubility of this molecule [6]. Therefore, these molecules can host non-polar compounds by a "host-guest" mechanism, improving the solubility and bioavailability of drugs [7,8]. The versatility of this group of oligosaccharide carriers justifies its wide application [9], such as for gene therapy devices [10,11].

Anterior studies reported low complexation efficiency of BNZ with some kinds of CDs, including β-cyclodextrin (β-CD) [12,13]. Limited aqueous solubility of natural CDs (α-CD,β-CD and γ-CD) is solved by using CD derivatives, such as hydroxypropyl-β-cyclodex-

* Corresponding author.
Email addresses: polyanne_melo86@yahoo.com.br (P.N. de Melo); euzebiogb@gmail.com (E.G. Barbosa); garneroc@fcq.unc.edu.ar (C. Garnero); liliabasiliocaland@gmail.com (L.B. de Caland); adleyantonini@yahoo.com.br (P.e.t.a.A.A.N.deLimaA.A.N. de Lima); mpedrosa@ufrnet.br (M.F. Fernandes-Pedrosa); mrlcor@fcq.unc.edu.ar (M.R. Longhi); arnobiosilva@gmail.com (A.A. da Silva-Júnior)

http://dx.doi.org/10.1016/j.molliq.2016.08.042
0167-7322/

trin (HP-β-CD), which exhibit greater solubilizing power, low cost, and low toxicity [14]. In some cases, CD complexation, even with CD derivatives, does not provide a suitable amount of soluble drug. Thus, the association of a third compound in these inclusion complexes has demonstrated an interesting approach with extraordinary results [15,16]. These ternary complexes are supramolecular aggregates generally composed of a drug, CD, and a third compound, which have several origins and proposals [17].

The solubilizing ability of 2-pyrrolidone and derivatives such as 1-methyl-2-pyrrolidone (NMP) for different non-polar drugs occurs by complexation or cosolvency mechanism [18,19]. However, these substances still have not been used in ternary complexes with CDs. On the contrary, triethanolamine (TEA) has been successfully used in association with CD for this purpose [20,21]. Recently, we have demonstrated that TEA significantly increased methotrexate affinity for β-CD, stabilizing MTX-β-CD interaction, leading to the attainment of solid ternary complexes with higher drug solubility and faster *in vitro* drug dissolution for potential use in psoriasis treatment [22].

BNZ is an unusual non-polar molecule. Previous studies demonstrated that cosolvent TEA competed with BNZ for the β-CD cavity at low concentrations, decreasing the complexation efficiency [23]. Hence, the purpose of this study was to establish the mechanism whereby the hydrophilic compounds (TEA and NMP) work with HP-β-CD to increase the solubility of BNZ. The experimental approach focused on the assessment and explanation of the self-assembling in aqueous phase by using phase solubility diagrams, molecular modeling, and nuclear magnetic resonance (^{1}H RMN) studies. In addition, the possible maintenance of these interactions in solid complexes was assessed for solid complexes prepared by spray drying and physical mixing. The way whereby the structural changes also affect the performance of *in vitro* drug dissolution was also carefully examined.

2. Materials and methods

2.1. Materials

BNZ, *N*-benzyl-2-(2-nitroimidazol-1-yl) acetamide (99.33%), was donated by Pharmaceutical Laboratory of Pernambuco-Brazil (LAFEPE®); HP-β-CD was purchased from Trappsol® (U.S.A.), TEA was purchased from Synth (Brazil), and NMP was purchased from Vetec (Brazil). All other reagents were analytical grade. The purified water (1.3 μS) was prepared from reverse osmosis purification equipment, model OS50 LX, Gehaka (Brazil).

2.2. Phase solubility studies

An excess of BNZ was added to flasks containing different HP-β-CD concentrations (0 to 0.14 mol L^{-1}) in water (binary complex), in the presence of 10% w/v (0.67 mol L^{-1}) of TEA or 10% w/v (0.025 mol L^{-1}) of NMP (ternary complexes). All flasks were hermetically closed and maintained in a thermostatic bath at 25.0 ± 2.0 °C for 72 h, and shaken in ultrasonic bath for 15 min, every 12 h. Afterwards, the suspensions were filtered through 0.45 μm membrane filters of cellulose acetate (Sartorius® Biolab Products, Germany), the pH of each solution was measured, and BNZ concentration was analytically determined by using UV spectrophotometry at 324 nm, previously validated [23]. The experimental results were expressed as the mean values of three replicates (n = 3). The apparent stability constants (K_c) of BNZ:HP-β-CD complexes were estimated using a fitted plot of a solubility diagram, according to the following equation: $K_c = slope / S_o$ (*1-slope*), where S_o is the drug solubility in absence of HP-β-CD and slope was extracted from the fitted phase solubility diagrams, assuming 1:1 stoichiometry [24].

2.3. Job's plot method

The complex stoichiometry between BNZ and the studied CD was also assessed by Job's method of continuous variation [25]. Solutions of BNZ and HP-β-CD were prepared at 0.115 mM and the UV–vis spectra were recorded for different solutions containing the same total molar content (BNZ + CD), but varying the ratio between them. The difference of absorbance at 324 nm between the solutions without and with CD were plotted (Δabs × [BNZ]) in function of *R* (*R* = [BNZ] / [BNZ] + [CD]). Each absorbance spectra was expressed as the mean of three replicates. The same assay was performed for the ternary complexes, in which the CD solutions were prepared mixed with TEA (0.67 mol L^{-1}) or mixed with NMP (0.025 mol L^{-1}).

2.4. Molecular modeling

Molecular dynamic simulations were performed by using the GROMACS package [26]. Binary (BNZ:HP-β-CD) and ternary interactions (BNZ:HP-β-CD:TEA; BNZ:HP-β-CD:NMP) were investigated in water, at atomic level by placing non-interacting molecular models for BNZ and HP-β-CD in randomly dispersed third compounds. Explicit SPC/E water models were used in a triclinic box with the adequate concentration of TEA and NMP. The molecular gromos53a6 topologies were created by using the Automated Topology Builder (ATB) and Repository version 2.0 [27]. The topologies were manually curated. Prior to molecular dynamic simulation, the geometries were optimized with energy minimization using the steepest descent algorithm, followed by conjugated gradient minimization. Two prior stabilization simulations were performed at 100 ps using NVT and then NPT ensembles at 300 K to gently relax the water molecules and for the stabilization of the box density. Unrestrained molecular dynamics were then performed at 310 K and 1.0 bar for 20 ns (2 fs time step). Temperature was coupled with rescaling velocities and pressure with isotropic pressure bath and Parrinello-Rahman barostat. The covalent bonds were constrained using the LINCS algorithm. The short-range interaction was computed until 8 Å. The Particle Mesh Ewald was used to simulate electrostatic beyond the cut-off, and Lennard-Jones interactions were disregarded outside the cut-off volume.

The molecular dynamic simulations were analyzed using the USCF chimera software [28]. The MD analysis module was employed to cluster the most significant and prevalent conformations for the system. Energy involved in the interactions was evaluated using GROMACS energy module. The short-range Lennard-Jones interaction energies between BNZ and HP-β-CD were plotted to pinpoint complex formation. All molecular visualization was also provided by USCF chimera software.

2.5. ^{1}H Nuclear magnetic resonance (NMR) studies

All experiments were performed on a Bruker Avance II High Resolution Spectrometer, equipped with a Broad Band Inverse probe (BBI) and a Variable Temperature Unit (VTU). All experiments were conducted at 298 K, using 5 mm sample tubes. The NMR data were processed with the MestReNova software (version 6.0.2-5475). NMR spectra were taken in D_2O. The D_2O 99.9 atom% D (Sigma, Aldrich® Co-Saint Louis, USA) was used in spectroscopic studies at 400.16 MHz. The chemical shifts (δ) were reported as ppm, and the residual solvent signal (4.80 ppm) was used as the internal reference. Induced changes in the ^{1}H NMR chemical shifts (Δδ) for BNZ and

HP-β-CD occurring due to the complexation were calculated according to the following equation: $\Delta\delta = \delta_{complex} - \delta_{free}$. The concentration of compounds was 0.015 mol L^{-1}.

2.6. Solid sample preparation

Spray-dried (SD) solid complexes were produced by using 50 mL ethanol:water (50:50 v/v) solutions containing equimolar amount ratios of 1:1 for the binary complex (BNZ:HP-β-CD), and 1:1:1 for ternary complexes (BNZ:HP-β-CD:TEA or BNZ:HP-β-CD:NMP). These different solutions were spray dried in a Buchi Mini Spray Dryer, (model B-191) in established drying conditions, with a feed flow of 5.0 mL min^{-1} and an inlet temperature of 120 °C. Pure BNZ was also dried using the same conditions, in order to check the influence of the drying conditions on the crystallinity of drug. The particles were collected and stored in a desiccator at room temperature for further characterization. The same ratio for compounds was uniformly mixed into a mortar to produce solid complexes prepared by physical mixture (PM). These PM ternary complexes were prepared firstly by mixing the BNZ and HP-β-CD to obtain a very homogeneous mixture of powders, and then the co-solvent (TEA or NMP) was added and mixed until the formation of a homogeneous mass, giving a damp appearance and with clumps to the samples.

2.7. Physicochemical aspects of solid complexes

Drug loading was assessed by UV–vis spectrophotometry at 324 nm, and the methodology used was previously validated [23]. Suitable amounts of samples were dissolved in aqueous solution of ethanol 20% (v/v) and then diluted in water to obtain a BNZ concentration of 20 μg mL^{-1}. The mean drug concentration was calculated by the straight-line equation from a standard curve fitted plot (n = 3).

Fourier Transform Infrared Spectroscopy (FTIR) was applied to all pure compounds, and SD and PM samples with the same composition. All analyses were performed at room temperature, in the range of 400–4000 cm^{-1}, by using KBr pellets (2.0 mg of sample per 300.0 mg of dried KBr) in a Perkin Elmer 65 FTIR spectrometer. The spectra for PM and SD samples were compared using an *ad hoc* algorithm capable of pinpointing the regions with larger deviations [29]. This algorithm divides two spectra into two equal parts and computes a correlation of the transmittance values between them. These correlation values (r) are attributed to a vector with the same size of the subdivided spectra. The process is repeated for ever-increasing spectral subdivisions. The final correlation vector (presented atop the spectra being compared) is the mean of all the computations. This vector gives peaks pointing to where two spectra are most dissimilar. It is usual to set a level between 0.80 and 1.00 to indicate high correlation, and values < 0.50 indicate a low correlation. The noisy baseline was discarded and only the regions with peaks were considered for correlation in the analysis.

X-ray diffraction analysis (XRD) was carried out for different samples in a Rigaku Miniflex II diffractometer with a Dtex ultra detector. The samples were analyzed in the 2θ angle range of 5° to 45° using Cukα radiation (λ = 1.54 Å). The XRD patterns were recorded under room temperature conditions in triplicate.

The shape and aspect of particles were investigated through scanning electronic microscopy (SEM) (ESEM, XL 30 Philips). The particles were dried and mounted on metal subs using double-sided adhesive carbon tape with conductive effect and then coated with a thin layer of gold in a Sputter Coater, and analyzed with SEM at a voltage of 20.0 kV.

2.8. In vitro drug release studies

In vitro dissolution studies were carried out according to The Food and Drug Administration [30] and the United States Pharmacopoeia [31] on a USP 30 apparatus 2, with a Hanson SRII 6 Flask Dissolution Test Station (Hanson Research Corporation, Chatsworth, USA). Samples containing 10 mg of BNZ in hard gelatin capsules (n^o 3) were placed into 500 mL of hydrochloric acid solution (HCl 0.1 N, pH = 1.2) at 37 °C, at 75 rpm. At specific intervals, 2 mL of dissolution medium was collected, filtered through a 0.45 μm cellulose acetate membrane and analyzed by UV–vis spectrophotometry at 324 nm (n = 3).

Data of cumulative drug amount *versus* time were mathematically adjusted by Higuchi Equation in order to compare different velocity constants (K_H). In addition, some parameters such as Q_{30min} and Q_{60min} (amount of dissolved drug at 30 and 60 min), and DE_{30} and DE_{60} (dissolution efficiency at 30 and 60 min) were also considered. The latter was determined using area under curve dissolution in the specific interval time ($ASC_{0–30}$ and $ASC_{0–60}$) with the trapezoidal rule [32].

2.9. Statistics

Similar data of distinct ternary complexes were subjected to Student-*t*-test for pairwise comparisons to identify the better third compound (TEA or NMP). A $p < 0.05$ was required for significance.

3. Results and discussion

3.1. Phase solubility studies

Fig. 1A shows the BNZ:HP-β-CD phase solubility diagrams (i) in water, (ii) in 0.670 mol L^{-1} of TEA, and (iii) in 0.025 mol L^{-1} of NMP. A_L type phase solubility diagrams for the BNZ in different HP-β-CD concentrations were identified in all three cases. The r values (> 0.95) demonstrated the linear increase in the apparent aqueous solubility of BNZ according to HP-β-CD concentration, suggesting the formation of soluble complexes with 1:1 stoichiometry.

The K_c obtained in cases (i), (ii), and (iii) were 49.90 M^{-1}, 31.06 M^{-1}, and 29.19 M^{-1}, respectively. The K_c provides quantitative information according to the thermodynamic equilibrium established between the inclusion complex and free soluble compounds [33]. Therefore, the greater equilibrium was verified for case (i), followed by (ii) and (iii), showing some limitation to complex formation when adding the third compounds. The presence of TEA with HP-β-CD increased apparent aqueous solubility of BNZ about 5.9 ± 0.4 times, whereas the presence of NMP increased the solubility to 7.1 ± 0.2 times, in relation to water solubility of BNZ, both less than in the absence of the co-solvents (Table 1). The TEA and NMP contribute to increasing the BNZ solubility, but decreased the complexa-

Table 1
Summary of the findings from the phase solubility studies.

Solubility parameters	BNZ:HP-β-CD	BNZ:HP-β-CD:TEA	BNZ:HP-β-CD:NMP
Initial solubility (mg mL^{-1})[a]	0.20 ± 0.006	0.25 ± 0.02	0.51 ± 0.009
Maximum solubility (mg mL^{-1})	1.55 ± 0.28	1.21 ± 0.06	1.29 ± 0.02
Increment of solubility (times)	7.6 ± 1.5	5.9 ± 0.4	7.1 ± 0.2
Diagram type	A_L	A_L	A_L
K_c (M^{-1})	49.90	31.06	29.19

[a] BNZ solubility in absence of HP-β-CD, considering only the solvent medium.

tion efficiency with HP-β-CD. The detected differences between the three systems suggested that specific co-solvents interact with the drug and CD by different mechanisms or change the viscosity, conductivity, and surface tension of the aqueous medium [34]. Molecular dynamic simulations were performed to examine the BNZ:HP-β-CD complex formation in water and in presence of TEA or NMP. These results help to hypothesize the binding mode and relative affinity of BNZ for each system. Additionally, it was verified that the organic solvents have the ability to decrease the polarity of the aqueous complexation medium, leading to increased aqueous solubility of the drug (S_o) but decreasing K_c. This is due to the decreased tendency of the drug molecule to enter the cyclodextrin cavity with decreasing polarity of the complexation media, owing to the reduction of the dielectric constant [35]. This event can be seen in the present study when TEA and NMP were added to the aqueous complexation medium, even though a previous study showed that the K_c value for the fluasterone:HP-β-CD complex decreases with increasing ethanol concentration [35–37]. The initial BNZ aqueous solubility was increased by the TEA and NMP due to their cosolvency abilities. The NMP enhanced the drug aqueous solubility about 2.5 times, while with TEA the enhancement was 1.25 times (Table 1). It is known that the $\log P_{ow}$, which indicates the relationship between the solubility of the solvent in octanol and water, is directly related to the co-solvent ability [38]. The $\log P_{ow}$ values for NMP and TEA are, respectively, 1.21 and − 2.30, which explains the different solubility increases achieved for BNZ.

The K_c values observed for inclusion complex BNZ:HP-β-CD were lower than those observed for β-CD in the study performed by Melo et al. [23], which was 51.48 M^{-1}. This fact can be explained by the absence of substituents in the β-CD molecule, assuring an easy and more favorable interaction of the free hydroxyl groups with the imidazole group of BNZ molecule, through hydrogen bonds. Nevertheless, at the maximum concentration of HP-β-CD (0.14 mol L^{-1}) the apparent aqueous solubility of BNZ was higher (Table 1), when compared with BNZ:β-CD complex (< 2 times), which occurred because of the different physicochemical properties and greater aqueous solubility of HP-β-CD (about 600 mg mL^{-1}) compared with β-CD (about 18.5 mg mL^{-1}) [39,40].

3.2. Job's plot method

Job's plot method of continuous variation was also used to assess the stoichiometry involved in the formation of BNZ inclusion complex with HP-β-CD, with and without TEA and NMP. According to this method, the molar fraction of BNZ (R) relative to the maximum value of Δabs × [BNZ] represents graphically the stoichiometric proportion of the investigated inclusion complex. Fig. 1B demonstrates a highly symmetrical shape in the plot with the maximum value at R = 0.5, supporting the formation of the inclusion complex with 1:1 stoichiometry at distinct conditions, confirming the phase solubility diagrams. The shape of the plot provides qualitative insights about K_c, wherein strong binding affords a more angular plot resembling a perfect triangle, while a more balanced equilibrium demonstrates gentle curvature [41]. In the present study, a smooth curvature was identified for the three distinct complexes, although with different slopes, demonstrating the following order of K_c values: BNZ:HP-β-CD > BNZ:HP-β-CD:TEA > BNZ:HP-β-CD:NMP, corroborating with experimental observations in the phase solubility diagrams.

3.3. Molecular modeling studies

Molecular dynamic simulations of BNZ with CD permitted the observation of two stable binding modes (Fig. 2). In the first binding mode (1), the benzyl group of BNZ facing the major groove of HP-β-CD enabling one H-bond between the amide carbonyl and CD hydroxyl group. The nitro imidazole group stayed outside interacting with the solvent. The binding mode 2 proved to be a much more all-embracing interaction with more H-bonds formed with BNZ nitro and with amide moieties (nitrogen now as H-bond donor).

The presence of the third compound led to changes in BNZ-CD interactions (Fig. 3). The NMP competed strongly with BNZ for the HP-β-CD cavity, supporting the results observed in the *Job's plot* and phase solubility studies, wherein the K_c and increment of BNZ aqueous solubility were lower than the values found for BNZ:HP-β-CD binary complex, despite keeping the A_L type phase solubility, but with a lower slope of the line (Fig. 1). Previous studies reported the same competition of TEA with BNZ for the β-CD cavity [23]. However, this phenomenon was not observed in TEA and HP-β-CD, as a delay in the complexation step occurred possibly due to the cosolvent effect of TEA.

The NMP occupied the HP-β-CD cavity more easily, impairing the BNZ complexation. In the presence of this third compound the drug seems to interact only externally with HP-β-CD (Fig. 3). Observing the TEA effect, the third compound delayed the complexation, which occurred for only one encounter when compared with the binary complex. However, this event persisted until the end of the simulation, suggesting the stabilization of the formed complex. This same stabilizing effect of TEA was reported for the ternary complex of the anticancer drug methotrexate with β-CD [22].

3.4. ^1H NMR spectroscopic studies

The chemical shifts (δ) identified for BNZ and HP-β-CD protons, as well as the changes induced by interactions between the two compounds are shown in Table 2. Evidence of BNZ:HP-β-CD interactions in the binary and ternary complexes in aqueous solutions was based on changes of the NMR spectra of the mixtures compared with individual compounds. All BNZ protons showed shielding effects in the NMR spectra, suggesting that they are close to a host atom rich in

Table 2
^{1}HNMR chemical shifts (δ) of the individual compounds and changes (Δδ) in the presence of the binary and ternary systems. See proton numbering in BNZ (A) and HP-β-CD (B).

A

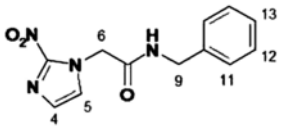

B

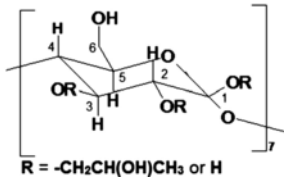

R = -$CH_2CH(OH)CH_3$ or H

Assignment	δ_{free}	Δδ		
		BNZ:HP-β-CD	BNZ:HP-β-CD:TEA	BNZ:HP-β-CD:NMP
BNZ				
H_4	7.3221	− 0.0145	− 0.0505	− 0.0398
H_5	7.5416	− 0.0007	− 0.0400	− 0.0268
H_{11}	7.4816	− 0.0134	− 0.0462	− 0.0414
H_{12}–H_{13}	7.4158	− 0.0123	− 0.0619	− 0.0465
HP-β-CD				
H_1	5.2564	0.0297	− 0.0011	0.0119
H_2	3.6361	0.0243	− 0.0156	0.0163
H_3	4.0207	0.0091	0.0153	0.0087
H_4	3.5268	0.0120	− 0.0173	Overlap
H_5	3.7386	0.0234	0.0803	0.0095
H_6	3.8999	0.0124	0.0217	− 0.0048
CH_3	1.1782	0.0109	− 0.0235	− 0.0087

π-electrons, possibly due to their association with oxygen atoms of HP-β-CD, confirming the complexation. Identified deshielding for distinct BNZ protons H_4, H_5 and H_{11}, H_{12}-H_{13} indicated the possible conformer with inclusion of the benzyl portion of the molecule inside HP-β-CD, as suggested in dynamic simulations (Fig. 2). The NMR spectrum of the binary complex showed that HP-β-CD protons exhibited deshielding induced by interactions with BNZ, particularly H_3 and H_5 shifts, suggesting that BNZ penetrates partially into the cavity from the wider side. Nevertheless, due to the deshielding effect of the external protons in the presence of the guest, we cannot exclude a probable interaction between BNZ and the outer surface of HP-β-CD, as demonstrated in dynamic simulations in the presence of NMP (Fig. 3).

More pronounced shifts for BNZ protons in the ternary associations allowed us to postulate that BNZ formed a ternary complex with HP-β-CD and TEA. Furthermore, HP-β-CD protons were significantly affected in the ternary BNZ:HP-β-CD:TEA sample. The H_3 and H_5 (located within the CD cavity) and the H_6 (located in the narrow border) protons showed deshielding shifts, occurring due to the possible partial inclusion of an electronegative group. The value of $\Delta\delta H_5$ confirmed observations of binary complexes that BNZ penetrates partially into the HP-β-CD cavity from the wider side. Shielding displacement identified for protons of the external surface of CD allowed us to postulate that TEA interacts with the external hydroxyl groups of HP-β-CD, as observed in the dynamic simulations (Fig. 3) stabilizing drug interaction with CD and forming a ternary complex.

Less pronounced changes in the HP-β-CD signals in the ternary BNZ:HP-β-CD:NMP sample, specifically internal H_3 and H_5, point to reduced complexation. Shielding of protons located at the outer surface of HP-β-CD suggested a conformational rearrangement of host molecule. These results associated with observations in the phase diagrams and molecular modeling studies permitted the understanding of the real contribution of co-solvents TEA and NMP for BNZ complexation with HP-β-CD. In addition, different observations of self-assembling behavior of the involved compounds studied in aqueous phase permits the prediction and better explains the importance of these third compounds for the solid complexes.

3.5. Drug-CD interactions in the binary and ternary solid complexes

After establishing the mechanism whereby the selected third compounds interacted with BNZ in the ternary complexes with HP-β-CD in aqueous medium, solid complexes were prepared by using equimolar amount ratios of 1:1 for the binary complex (BNZ:HP-β-CD), and 1:1:1 for the ternary complexes (BNZ:HP-β-CD:TEA or BNZ:HP-β-CD:NMP). Spray-dried solid complexes were successfully produced using selected parameters, and a yellowish-white powder was gathered from the equipment collector. In addition, pure BNZ was also dried and used as control in the drug analysis. The drug assay for different samples demonstrated that BNZ was efficiently loaded in the binary and different ternary solid samples. Similar drug loading efficiency (Student-*t*-test, p = 1.00), superior to 94%, was observed for different complexes, compared with theoretical drug ratio. The high drug loading is characteristic of drug-loaded microparticles produced by using the spray-drying method [42–44]. The physical mixture solid complexes showed up as a loose white powder, but the ternary complexes presented some aggregates and a damp appearance, due to the presence of the co-solvent in liquid form. The drug loading of these complexes was about 100%, due to no loss of powder.

The FTIR spectra for pure compounds were monitored in the binary and ternary complexes prepared by both physical mixture (PM) and spray-drying (SD) methods. All of the bands observed in the FTIR spectra of HP-β-CD, BNZ, PM, and SD complexes can be seen in the Supplementary material (Fig. 1). Major changes in the spectra of complexes were recorded in the range of 400–1700 cm^{-1} (Fig. 4). More pronounced signals of HP-β-CD were observed, due to the larger mass/mass proportion in the samples. Major changes in the spectra of complexes were recorded in the range of 400–1700 cm^{-1}. Thus, the comparisons were made in this wave number range with that of the single compounds.

The N—H deformation in the FTIR spectra of BNZ was recorded at 1554 and 1536 cm^{-1}, while the characteristic carbonyl group stretching of amide was also observed at 1660 cm^{-1}. The N—C deformation, still with the amide, can be seen in the range of 1200 to 1000 cm^{-1}. The clusters of bands at 1418, 1486, and 1500 cm^{-1} were also observed, the latter two as an adjacent band due to the C—C bond stretch present in the aromatic ring. The bands at 1335 and 1291 cm^{-1} referred to the C—N bond stretch in the aromatic amines. The N—O bond stretch present in the NO_2 group was identified in the range of 1660 to 1500 cm^{-1} and 1365 to 1335 cm^{-1}(Fig. 4).

The O—H bond deformation and C—O stretching of secondary OH in the FTIR spectra of HP-β-CD were recorded in the region of 1420–1330 cm^{-1} and 1080 cm^{-1}, respectively. The C—H bond stretch of sp^3 carbons due to methyl groups (CH_3) was observed at 1373 cm^{-1} (Fig. 4). The characteristic H-O-H deformation band, observed for water molecules, was also observed at 1645 cm^{-1} [45], while cyclic ether O—C stretching was observed at 1150 cm^{-1}. The binary and ternary complexes prepared by PM exhibited an overlap of bands of pure compounds, giving evidence of weak interaction between BNZ and HP-β-CD. However, further analysis is necessary in order to confirm this hypothesis (Fig. 4).

In the comparisons of the computed *ad hoc* algorithms in Fig. 4, it was possible to notice sharp peaks on (A, B, C) proving that the main differences occurred mainly in the range of 1600 to 1400 cm^{-1}. This region corresponded to the absorption of nitro groups of BNZ, corroborating with the molecular modeling studies (Fig. 2). In addition, comparisons of BNZ:HP-β-CD:TEA SD with BNZ:HP-β-CD:TEA PM (B) and BNZ:HP-β-CD:NMP SD with BNZ:HP-β-CD:NMP PM systems (C) have demonstrated differences mainly in the range of 1200 to 1000 cm^{-1}. This region corresponds to the C—O stretching of the ether and alcohol grouping present in the HP-β-CD. In the liquid phase, the interaction of the BNZ benzyl ring with the carbonyl backbone of CD was observed. The N—C stretching of amide group of BNZ can also be seen in this region. The ^{1}H NMR spectroscopy and molecular modeling studies have also demonstrated H-bond formation between the amide carbonyl and CD hydroxyl group. Thus, FTIR results demonstrated that some interactions observed between CD and the guest molecule in liquid phase were also observed in the SD solid complexes, suggesting that at least part of the drug was complexed with the CD in the solid complexes.

3.6. Structural properties of particles

Aspects of the drying procedure, *e.g.*, the solvent and temperature, affect the crystalline habit of the drug [46–48]. The diffraction pattern of non-spray dried BNZ (NSD) (Fig. 5A) showed high-intense diffraction peaks at 2θ values of about 7.2, 10.8, 16.6, 21.8, and 25° with secondary peaks with smaller intensity, confirming the presence of crystalline form I in the sample [49]. The spray drying induced the reduction of peak intensity at 2θ values of 7.2, 10.8, 16.6, and 21.8°, and some amorphization. This was reinforced in the SEM images (Fig. 5B), in which BNZ NSD appeared as partially agglomerated regular crystals, while BNZ SD presented agglomerates of smaller particles [50–52]. The HP-β-CD revealed amorphous spherical parti-

cles. The presence of both third compounds (TEA and NMP) in PM samples seems not to affect the drug crystallinity in the particles, but some dissolution of the compounds occurring during the physical mixture procedure certainly altered the drug-CD interaction and the wettability of the solid particles, possibly improving the drug dissolution.

The XRD patterns for SD systems showed considerable drug amorphization, but the reflectance peaks confirmed that the whole part of BNZ was not complexed. The third compounds seemed to enhance the reorientation of the material, decreasing the efficiency of drug complexation during the drying, since the drug amorphization was higher in the binary SD complexes. The SEM images also demonstrated the regular spherical particles characteristic of spray-dried products, but the insets clearly demonstrated the presence of small needle-shaped crystals of the drug covering the surface of the binary and ternary spray-dried particles (Fig. 5B). These results proved that the spray-drying procedure was not able to produce amorphous ternary complexes. Sometimes, the drug distribution near the surface of the dried particles can occur in an amorphous state [43,44] because during the spray drying of molecular dispersions containing drug and macromolecules, the solvent evaporation induces a capillary flow, followed by faster diffusion of small molecules, into the matrix of particles, with the self-assembly of the drug near the surface of particles [53]. In the case of less soluble molecules, such as BNZ, the material adsorbs preferably on air/liquid interface before it turns into a dry particle [54,55], which explained the presence of BNZ crystals on SD particles. The presence of TEA and NMP in the samples increased this phenomenon.

Moreover, previous thermodynamic studies with BNZ inclusion complexes with β-CD have demonstrated an enthalpic barrier against drug-CD interaction and spontaneous formation of the inclusion complex [23]. Hence, the high temperature used during the spray drying (120 °C) seems to impair the easy drug-CD complexation, suggesting the considerable formation of solid dispersion among the compounds than the solid inclusion complex.

3.7. Dissolution studies

The XRD analyses and SEM images demonstrated that the procedure (SD or PM) used for preparing solid complexes showed distinct aspects of crystallinity and morphology of particles. This fact revealed different drug interactions of the drug with CD and third compounds. Thus, the effects of the composition and preparation procedure on the drug dissolution rate were separately compared, evaluated, and correlated with their physicochemical aspects. The non-spray dried BNZ (BNZ NSD) was compared with samples prepared by physical mixture (PM) (Fig. 6A), while the spray-dried drug (BNZ SD) was compared with that prepared by spray drying (SD) (Fig. 6B). In addition, all drug dissolution profiles were mathematically adjusted by the Higuchi equation: $BNZ\% = k_H\ t^{0.5}$, only to compare the rate constant (k_H) (Table 3).

The PM binary association exhibited a drug dissolution profile similar to that observed for BNZ NSD, which is in accordance with the FTIR, XRD, and SEM study, wherein the complex inclusion formation was not observed. This fact was additionally confirmed by the kinetic parameters, in which similar drug dissolution kinetic constants ($K_H \sim 10.5\%BNZ\ h^{0.5}$) were identified. Also, no differences were observed for the other dissolution parameters (Q_{30min}, Q_{60min}, DE_{30min}, and DE_{60min}). Furthermore, the presence of both third compounds TEA and NMP considerably enhanced the drug dissolution rate. In contrast to that observed in the studies in liquid phase, TEA and NMP showed similar effects: They doubled the drug dissolution rate ($K_H \sim 23.0\%BNZ\ h^{0.5}$) compared with BNZ NSD and binary PM association. The structural properties of particles and the studies performed in aqueous phase reinforced that this phenomenon occurred because the co-solvents improve the wettability and change the drug-CD interaction. The superior drug dissolution rate of the drug from ternary PM associations proved the importance of the selected co-solvents, and their ability to enhance the drug-CD interaction with water due to the cosolvency effect. The presence of these substances significantly affected the wettability of the particles, permitting the easer interaction of BNZ with HP-β-CD and reducing the drug dissolution time considerably.

The comparisons among the SD samples revealed the best performance for BNZ:HP-β-CD ($K_H \sim 11.5\%\ BNZ\ h^{0.5}$) followed by the BNZ:HP-β-CD:NMP SD ($K_H \sim 10.3\%\ BNZ\ h^{0.5}$) and BNZ:HP-β-CD:TEA SD ($K_H \sim 8.6\%\ BNZ\ h^{0.5}$), respectively. This fact was clearly confirmed when Q_{30min} was observed for the different samples (Table 3), which is explained by the highest drug amorphization observed for the binary SD sample in the XRD results (Fig. 5A). The presence of third compounds in the SD particles decreased the drug amorphization and consequently the ratio of the complexed drug, reducing the dissolution efficiency. Previous studies with acetylsalicylic acid have demonstrated a dependence on crystallite size according to the co-precipitation method used, in which the drug dissolution rate decreases according to the enhanced crystallinity of particles [56].

As explained in the XRD results, the spray drying was not able to induce the formation of totally amorphous solid dispersions. In addition, the co-solvents enhanced the crystallinity of the drug in the SD ternary association, explaining the best performance for the samples prepared by physical mixture. The high drying temperature (about 120 °C) easily decreased the drug-HP-β-CD interaction, inducing the formation of a solid dispersion containing the non-complexed molecules. Initially, only the crystal surface is accessible to the external environment of the particle, limiting the complete drug dissolution. A larger number of molecules with these lower aqueous solubility groups, *e.g.*, the phenyl ring of the BNZ molecule, facing the outer layer of the crystal may decrease the dissolution rate of the drug, due

Table 3
Dissolution parameters calculated for different samples (drug dissolved in 30 and 60 min [Q_{30min} and Q_{60min}], dissolution efficiency in 30 and 60 min [DE_{30min} and DE_{60min}] and velocity constants [K_H]).

Groups	Samples	$Q_{30min} \pm SD$ (%)	$Q_{60min} \pm SD$ (%)	$DE_{30min} \pm SD$ (%)	$DE_{60min} \pm SD$ (%)	$K_H \pm SD$ (%BZN $t^{0.5}$)
Non spray dried samples (NSD, PM)	BNZ NSD	61.7 ± 3.2	63.9 ± 6.5	38.6 ± 0.8	53.3 ± 2.4	10.29 ± 0.49
	BNZ:HP-β-CD PM	58.8 ± 8.0	85.1 ± 5.0	34.4 ± 4.6	54.0 ± 6.1	10.55 ± 1.10
	BNZ:HP-β-CD:TEA PM	94.7 ± 1.1	93.7 ± 1.8	76.8 ± 2.2	85.5 ± 0.7	22.99 ± 0.61
	BNZ:HP-β-CD:NMP M	94.7 ± 0.3	95.9 ± 0.8	80.2 ± 2.2	88.7 ± 0.8[a]	24.09 ± 0.65
Spray dried samples (SD)	BNZ SD	34.2 ± 7.7	45.7 ± 11.7	21.4 ± 3.3	31.0 ± 6.6	5.99 ± 1.29
	BNZ:HP-β-CD SD	78.5 ± 9.1	96.2 ± 2.7	34.7 ± 4.8	63.3 ± 4.0	11.88 ± 0.82
	BNZ:HP-β-CD:TEA SD	39.1 ± 0.6	82.8 ± 6.0	21.9 ± 1.0	42.6 ± 1.0	8.55 ± 0.27
	BNZ:HP-β-CD:NMP SD	57.7 ± 10.4	92.0 ± 8.4[b]	27.7 ± 3.8	52.8 ± 5.9	10.32 ± 1.08

At the 0.05 level, the difference of the means is significantly different with the [a] paired Student-*t*-test: BNZ:HP-β-CD:TEA PM *versus* BNZ:HP-β-CD:NMP PM and with the [b] paired Student-*t*-test: BNZ:HP-β-CD:TEA SD *versus* BNZ:HP-β-CD:NMP SD.

to the formation of a protective outer monolayer [57], as seen in the XRD and SEM studies. Furthermore, the rapid drying restricts particle growth after forming fine droplets, which induces agglomeration of the microparticles [58], and the molecules of the co-solvents TEA and NMP are differently distributed into the particles produced by spray drying, compared with those by physical mixture [59].

Previous studies reported that freeze-dried ternary complex acetazolamide:HP-β-CD:TEA was significantly better than the binary complex and the pure drug in the *in vitro* release studies [60], inducing higher drug bioaccessibility in the *in vitro* corneal permeability and bioavailability in the *in vivo* intraocular studies [61]. However, the same referred ternary complex exhibited a lower drug dissolution rate compared with the binary complex, due to the strong particle agglomeration [62], but not due to the exposure of the samples to high temperatures, as seen in spray drying. Thus, it can be confirmed that the TEA changes the interaction of the drug with CD, but this depends on the preparing procedure.

Although the spray drying technique is widely used to obtain inclusion complexes with many molecules of low aqueous solubility, this study proved that the use of high temperatures can modify the interaction between the host and guest molecules, due to thermodynamic inclusion properties, reducing the stability constant (K_c) [63,64]. Furthermore, the lower dissolution rate for SD samples could be due to a displacement of the BNZ molecules from the HP-β-CD cavity due to the fast solvent evaporation rate [65]. A previous study of solid-state NMR showed no spectral evidence of inclusion complex formation in physical mixtures of BZN with β-CD, HP-β-CD, and methyl-β-cyclodextrin (Me-β-CD) [40], which was in accordance with the dissolution results for binary PM associations in this study.

The results discussed in this approach clearly proved the importance of the co-solvents (TEA and NMP) to improve the drug dissolution performance from ternary complexes with HP-β-CD and established the mechanism whereby these substances worked together with the CD in a new and interesting raw material. The spray-drying procedure was not a procedure able to reproduce the dissolution performance identified in the samples prepared by physical mixtures.

4. Conclusion

Important new information about the influence of co-solvents NMP and TEA as third compounds were provided in the self-assembly BNZ:HP-β-CD associations in order to obtain a new raw material for oral BNZ delivery application in solid dosage form (tablets or powder) or extemporaneous suspensions. We have shown through molecular modeling studies two possible conformers with the inclusion of 2-nitroimidazolic or benzyl portion of molecule inside the cavity, which were confirmed in the NMR studies. These studies also clarified the results observed in the phase diagrams and Job's plot method, proving that NMP competed with BNZ for HP-β-CD. On the other hand, TEA seems to delay and stabilize the drug-CD interaction, forming a ternary complex. The solid phase studies have demonstrated distinct contributions of the selected co-solvents according to the drying method. In the PM ternary associations, the co-solvents increased the wettability, changing the drug-CD interaction and improving the drug dissolution. Although the SD solid associations showed spherical particles, the co-solvents decreased the drug-CD miscibility and complexation efficiency, forming mainly non-amorphous ternary solid dispersions. This fact was confirmed in the dissolution studies, in which the performance of both PM ternary associations (BNZ:HP-β-CD:NMP and BNZ:HP-β-CD: TEA) was substantially higher than binary associations and SD samples. Thus, the synergistic enhancement of BNZ dissolution occurred with the co-solvents in PM ternary solid phase, supporting the importance of these substances in the enhancement of the HP-β-CD effect. The simple physical mixture of the drug, CD, and a specific cosolvent can significantly increase the drug dissolution rate, without using more costly methods to achieve a successful outcome. Moreover, the spray drying was not a suitable method for preparing the specific ternary complex, suggesting the use of cold drying methods.

Supplementary data to this article can be found online at http://dx.doi.org/10.1016/j.molliq.2016.08.042.

Acknowledgements

The authors wish to thank the Brazilian National Council for Scientific and Technological Development (CNPq) for financial support (grant numbers: 483073/2010-5; 481767/2012-6) and Coordination for the Improvement of Higher Level (CAPES) (grant number: AUXPE no PNPD 23038.007487/2011-91 and scholarship of de Melo, P.N and de Caland, LB). The authors also acknowledge the help extended by Andy Cumming in proofreading the English text.

References

[1] J.A. Castro, M.M. Mecca, L.C. Bartel, Hum. Exp. Toxicol. 25 (2006) 471–479.
[2] J.R. Coura, J. Borges-Pereira, Rev. Soc. Med. Trop. 45 (2012) 286–296.
[3] World Health Organization (WHO), "Chagas disease (American trypanosomiasis)" Who fact sheet, media centre, n. 340, in: http://www.who.int/mediacentre/factsheets/fs340/en/, March 2015. Access: 07 May, 2015.
[4] L. Streck, M.M. Araújo, I. Souza, M.F. Fernandes-Pedrosa, E.S.T. Egito, A.G. Oliveira, A.A. Silva-Júnior, J. Mol. Liq. 196 (2014) 178–186.
[5] C.M. Lamas, L. Villaggi, I. Nocito, G. Bassani, D. Leonardi, F. Pascutti, Int. J. Pharm. 307 (2006) 239–243.
[6] S.V. Kurkov, T. Loftsson, Int. J. Pharm. 453 (2013) 167–180.
[7] L. Dong, M. Liu, A. Chen, Y. Wang, D. Sun, J. Mol. Liq. 177 (2013) 204–208.
[8] A. Stepniak, S. Belica-Pacha, S. Rozalska, J. Dlugonski, P. Urbaniak, B. Palecz, J. Mol. Liq. 211 (2015) 288–293.
[9] L. Jiang, Y. Yan, J. Huang, Adv. Colloid Interf. Sci. 169 (2011) 13–25.
[10] A.M. O'Mahony, S. Desgranges, J. Ogier, A. Quinlan, M. Devocelle, R. Darcy, Pharm. Res. 30 (2013) 1086–1098.
[11] V. Wintgens, C. Leborgne, S. Baconnais, V. Burckbuchler, E.L. Cam, D. Scherman, A. Kichler, C. Amiel, Pharm. Res. 29 (2012) 384–396.
[12] J.L. Soares-Sobrinho, M.F.L.R. Soares, P.J. Rolim-Neto, J.J. Torres-Labandeira, J. Therm. Anal. Calorim. 106 (2010) 319–325.
[13] J.L. Soares Sobrinho, M.F.L.R. Soares, J.J.T. Labandeira, L.D.S. Alves, P.J. Rolim Neto, Quim Nova 34 (2011) 1534–1538.
[14] Y. Zhang, K. Ren, Z. He, H. Li, T. Chen, Y. Lei, S. Xia, G. He, Y. Xie, Y. Zheng, X. Song, Carbohydr. Polym. 98 (2013) 638–643.
[15] M.K. Anwer, S. Jamil, M.J. Ansari, R. Al-Shdefat, B.E. Ali, M.A. Ganaie, M.S. Abdel-Kader, F. Shakeel, J. Mol. Liq. 199 (2014) 35–41.
[16] H. Bera, S. Chekuri, S. Sarkar, S. Kumar, N.B. Muvva, S. Mothe, J. Nadimpalli, J. Mol. Liq. 215 (2016) 135–143.
[17] S.V. Kurkov, T. Loftsson, Int. J. Pharm. 453 (2013) 167–180.
[18] A. Jouyban, V. Panahi-Azar, F. Khonsari, J. Mol. Liq. 160 (2011) 14–16.
[19] Y. Miyako, N. Khalef, K. Matsuzaki, R. Pinal, Int. J. Pharm. 393 (2010) 48–54.
[20] C. Garnero, M. Longhi, Anal. Chim. Acta 659 (2010) 159–166.
[21] G. Granero, C. Garnero, M. Longhi, Eur. J. Pharm. Sci. 20 (2003) 285–293.
[22] J.A.A. Barbosa, A. Zoppi, M.A. Quevedo, P.N.M. Melo, A.S.A. Medeiros, L. Streck, A.G. Oliveira, M.F. Fernandes-Pedrosa, M.R. Longhi, A.A. Silva-Júnior, Int. J. Mol. Sci. 15 (2014) 17077–17099.
[23] P.N. Melo, E.G. Barbosa, L.B. Caland, H. Carpegianni, C. Garnero, M. Longhi, M.F. Fernandes-Pedrosa, A.A. Silva-Júnior, J. Mol. Liq. 186 (2013) 147–156.
[24] T. Higuchi, K.A. Connors, Adv. Anal. Chem. Instrum. 4 (1965) 117–212.
[25] P. Job, Ann. Chim. Appl. 9 (1928) 113–203.
[26] S. Pronk, S. Páll, R. Schulz, P. Larsson, P. Bjelkmar, R. Apostolov, M.R. Shirts, J.C. Smith, P.M. Kasson, D. van der Spoel, B. Hess, E. Lindahl, Bioinformatics 29 (2013) 845–854.
[27] A.K. Malde, L. Zuo, M. Breeze, M. Stroet, D. Poger, P.C. Nair, J. Chem, Theory Comput. 7 (2011) 4026–4037.
[28] E.F. Pettersen, T.D. Goddard, C.C. Huang, G.S. Couch, D.M. Greenblatt, E.C. Meng, J. Comput. Chem. 25 (2004) 1605–1612.
[29] M.A.V. Pereira, G.D. Fonseca, A.A. Da Silva-Júnior, M.F. Fernandes-Pedrosa, M.F.V. Moura, E.G. Barbosa, J. Therm. Anal. Calorim. 116 (2014) 1091–1100.
[30] F.D.A., Food and Drug Administration, Center Drug Evaluation and Research. (CDER) Rockville, 1996.
[31] USP 30-NF 25, Rockville: United States Pharmacopeial Convention, 2007.
[32] K.A. Khan, C.T. Rhodes, Pharm. Acta Helv. 47 (1972) 14.

[33] T. Loftsson, D. Hreinsdóttir, M. Másson, Int. J. Pharm. 302 (2005) 18–28.
[34] P. Tonglairoum, T. Ngawhirunpat, T. Rojanarata, R. Kaomongkolgit, P. Opanasopit, Pharm. Res. 8 (2014). 1893-90.
[35] T. Loftsson, M.E. Brewster, J. Pharm. Sci. 101 (2012) 3019–3032.
[36] P. Li, L. Zhao, S.H. Yalkowsky, J. Pharm. Sci. 88 (1999) 1107–1111.
[37] Y. He, P. Li, S.H. Yalkowsky, Int. J. Pharm. 264 (2003) 25–34.
[38] A.S.A. Medeiros, A. Zoppi, E.G. Barbosa, J.I.N. Oliveira, M.F. Fernandes-Pedrosa, M.R. Longhi, A.A. da Silva-Júnior, Carbohydr. Polym. 20 (2016) 1040–1051.
[39] M.E. Brewster, T. Loftsson, Adv. Drug Deliv. Rev. 59 (2007) 645–666.
[40] J. Priotti, M.J.G. Ferreira, M.C. Lamasa, D. Leonardia, C.J. Salomona, T.G. Nunes, Carbohydr. Polym. 131 (2015) 90–97.
[41] J.S. Renny, L.L. Tomasevich, E.H. Tallmadge, D.B. Collum, Angew. Chem. Int. Ed. Eng. 52 (2013) 11998–12013.
[42] A.A. Silva-Júnior, M.V. Scarpa, K.C. Pestana, L.P. Mercuri, J.R. Matos, A.G. Oliveira, Thermochim. Acta 467 (2008) 91–98.
[43] A.R. Oliveira, E.F. Molina, P.C. Mesquita, J.L.C. Fonseca, G. Rossanezi, M.F.F. Pedrosa, A.G. Oliveira, A.A. Da Silva-Júnior, J. Therm. Anal. Calorim. 112 (2013) 555–565.
[44] P.C. Mesquita, A.R. Oliveira, M.F.F. Pedrosa, A.G. Oliveira, A.A. Da Silva-Júnior, J. Phys, Chem. Solids 81 (2015) 27–33.
[45] P.R.K. Mohan, G. Sreelakshmi, C.V. Muraleedharan, R. Joseph, Vib. Spectrosc. 62 (2012) 77–84.
[46] M. Asada, H. Takahashi, H. Okamoto, H. Tanino, K. Danjo, Int. J. Pharm. 270 (2004) 167–174.
[47] S.P. Velaga, S. Bergh, J. Carlfors, Eur. J. Pharm. Sci. 21 (2004) 501–509.
[48] N. Rajendiran, R.K. Sankaranarayanan, J. Mol. Liq. 206 (2015) 218–227.
[49] S.B. Honorato, J.S. Mendonça, N. Boechat, A.C. Oliveira, J. Mendes Filho, J. Ellena, Spectrochim. Acta A 118 (2014) 389–394.
[50] L. Brügemann, E.K.E. Gerndt, Nucl. Inst. Methods Phys. Res. A 531 (2004) 292–301.
[51] A.W. Burton, K. Ong, T. Rea, I.Y. Chan, Microporous Mesoporous Mater. 117 (2009) 75–90.
[52] A.L. Patterson, Phys. Rev. 56 (1939) 978–982.
[53] A.B.D. Nandiyanto, K. Okuyama, Adv. Powder Technol. 22 (2011) 1–19.
[54] C. Dahlberg, A. Millqvist-Fureby, M. Schuleit, M., Eur. J. Pharm. Biopharm. 70 (2008) 478–485.
[55] A. Millqvist-Fureby, P. Smith, Food Hydrocoll. 21 (2007) 920–927.
[56] G. Torrado, S. Fraile, S. Torrado, S. Torrado, Int. J. Pharm. 166 (1998) 55–63.
[57] R.H. Muller, C.M. Keck, J. Biotechnol. 113 (2004) 151–170.
[58] A. Fini, F. Ospitali, G. Zoppetti, N. Puppini, Pharm. Res. 25 (2008) 2030–2040.
[59] Y. Lu, N. Tang, R.L.J. Qi, W. Wu, Int. J. Pharm. 465 (2014) 25–31.
[60] G.E. Granero, M.M. Maitre, C. Garnero, M.R. Longhi, Eur. J. Med. Chem. 43 (2008) 464–470.
[61] S.D. Palma, L.I. Tartara, D. Quinteros, D.A. Allemandi, M.R. Longhi, G.E. Granero, Chem. Rev. 98 (2009) 2035–2044.
[62] M.J. Mora, L.I. Tártara, R. Onnainty, S.D. Palma, M.R. Longhi, G.E. Granero, Carbohydr. Polym. 98 (2013) 380–390.
[63] M.V. Rekharsky, Y. Inoue, Chem. Rev. 98 (1998) 1875–1917.
[64] J.J. Passos, F.B. Sousa, I.M. Mundim, R.R. Bonfim, R. Melo, A.F. Viana, E.D. Stolz, M. Borsoi, S.M.K. Rates, R.D. Sinisterra, Chem. Eng. J. 228 (2013) 345–351.
[65] A.R. Hedges, Chem. Rev. 98 (1998) 2035–2044.